Mechanosensitive Fluorescent Probes to Image Membrane Tension in Mitochondria, Endoplasmic Reticulum, and Lysosomes

Goujon, Antoine; Colom Diego, Adai; Strakova, Karolina; Mercier, Vincent; Mahecic, Dora; Manley, Suliana; Sakai, Naomi; Roux, Aurélien; Matile, Stefan

How to cite

GOUJON, Antoine et al. Mechanosensitive Fluorescent Probes to Image Membrane Tension in Mitochondria, Endoplasmic Reticulum, and Lysosomes. In: Journal of the American Chemical Society, 2019, vol. 141, n° 8, p. 3380–3384. doi: 10.1021/jacs.8b13189

This publication URL: https://archive-ouverte.unige.ch/unige:114631

Publication DOI: 10.1021/jacs.8b13189

Mechanosensitive Fluorescent Probes to Image Membrane Tension in Mitochondria, Endoplasmic Reticulum and Lysosomes

Antoine Goujon,[†,‡,§] Adai Colom,[†,‡,§] Karolína Straková,[†,‡] Vincent Mercier,[†,‡] Dora Mahecic,[‡,#] Suliana Manley,[‡,#] Naomi Sakai,[†,‡] Aurélien Roux*,[†,‡] and Stefan Matile*,[†,‡]

[†]School of Chemistry and Biochemistry, University of Geneva, CH-1211 Geneva, Switzerland

[‡]National Centre of Competence in Research (NCCR) Chemical Biology

[#]Institute of Physics, École Polytechnique Fédérale de Lausanne (EPFL), CH-1015 Lausanne, Switzerland

[§]These two authors contributed equally

ABSTRACT. Measuring forces inside cells is particularly challenging. With the development of quantitative microscopy, fluorophores which allow the measurement of forces became highly desirable. We have previously introduced a mechanosensitive flipper probe, which responds to the change of plasma membrane tension by changing fluorescence lifetime and thus allows tension imaging by FLIM. Herein, we describe the design, synthesis, and evaluation of flipper probes that selectively label intracellular organelles, i.e., lysosomes, mitochondria, and the endoplasmic reticulum. The probes respond uniformly to osmotic shocks applied extracellularly, thus confirming sensitivity toward changes in membrane tension. At rest, different lifetimes found for different organelles relate to known differences in membrane organization rather than membrane tension and allow co-labeling in the same cells. At the organelle scale, lifetime heterogeneity provides unprecedented insights on ER tubules and sheets, and nuclear membranes. Examples on endosomal trafficking or increase of tension at mitochondrial constriction sites outline the potential of intracellularly targeted fluorescent tension probes to address essential questions that were previously beyond reach.

The importance of mechanical forces in biological processes is only starting to emerge.[1–3] Plasma membrane tension is a topic of particular current interest because mounting evidence suggests its involvement in regulating various biochemical processes in cells.[2] Although membrane tension should also regulate membranous organelles' functions, standard techniques of force measurements, such as optical tweezers or force microscopes are difficult to apply inside of cells.[3] Therefore, the role of membrane tension in

organelles is so far poorly explored and awaits the development of non-invasive measurement methods.[1–4]

Responding to the need in mechanobiology, this study aimed at developing organelle-specific mechanophores based on the recently introduced fluorescent membrane tension reporter **1** (referred to as Flipper-TR® or FliptR, Figure 1).[5] This planarizable push-pull probe is composed of two dithienothiophenes (DTTs)[6] "flippers".[7] They are twisted out of co-planarity by repulsion between methyl groups and the σ holes[8] on the endocyclic sulfurs next to the bond connecting the DTTs. Sulfides and sulfones in the DTT bridges supported by a chalcogen-bonding[8] ether donor and a cyano acceptor serve as push and pull components.

In lipid bilayers, Flipper-TR® **1** responds to the increasing membrane order by planarization in the ground state, which results in red-shifted excitation maxima and longer fluorescence lifetimes.[5] Such properties are unique[9] among the membrane probes,

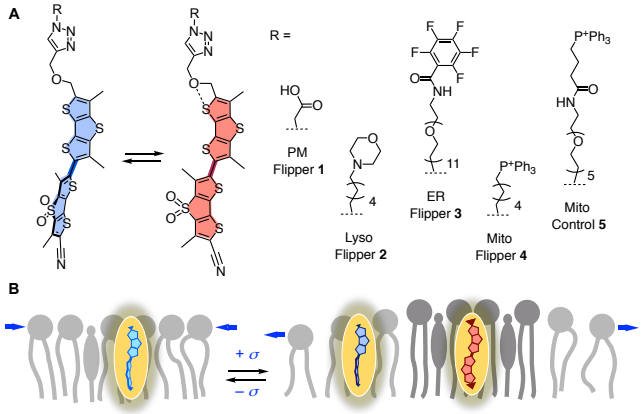

Figure 1. (A) Structure of Flipper-TR® **1**, Lyso, ER, and Mito Flippers **2**–**4**, and Mito control **5**. (B) With increasing membrane tension (right), the appearance of ordered domains (dark gray) causes an increase of fluorescence lifetimes, whereas the complementary domain disassembly (left) accounts for decreasing lifetimes with decreasing tension.

that usually report off-equilibrium in the excited state on viscosity or polarity.[9–16] In cellular membranes, the mechanophore **1** reports the increasing membrane order upon application of membrane tension σ by increasing fluorescence lifetime τ. This change was attributed to the formation of more ordered microdomains under membrane tension, due to the increased line tension between the stretchable and unstretchable lipid phases (Figure 1B, dark gray).[5,17] Roughly linear positive τ-σ correlations found with all tested cells demonstrated the applicability of **1** to measure membrane tension change by fluorescence lifetime imaging microscopy (FLIM).[5,18]

The headgroup of flipper **1** contains an essential triazole and a carboxylate to target the plasma membrane (PM; Figure 2C).[19] We have shown that the carboxylate can be replaced without loss of function by a boronic acid[20] and a biotin[21] to target ganglioside-enriched lipid domains and biotinylated targets on cell surfaces, respectively. Thus, probes **2**–**5** were designed incorporating established motifs from the respective trackers (Figure 1A).[12-16] Namely, Lyso Flipper **2** was equipped with a basic morpholine (pK_a 8.4) and a short hydrophobic linker to produce membrane-binding cationic amphiphiles only after protonation within the acidic late endosomes and lysosomes.[13,14] In Mito Flipper **4**, the same short linker is used to install a hydrophobic triphenylphosphonium cation for selective targeting of mitochondria with strong inside negative membrane potential.[13,15] ER Flipper **3** contains a pentafluorophenyl group to react with thiols in ER-membrane proteins, and

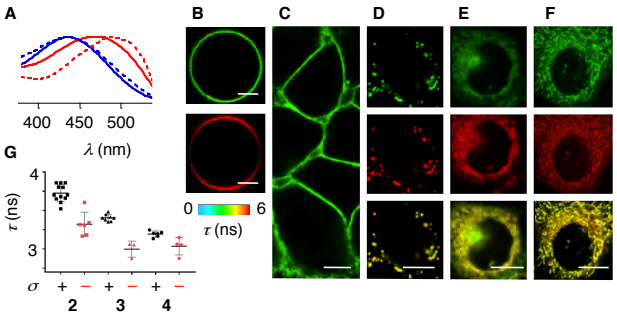

Figure 2. (A) Excitation spectra (λ_{em} 570 nm) of **1** (dashed) and **3** (solid) in L_d (blue, 1,2-dioleoyl-*sn*-glycero-3-phosphocholine: DOPC) and S_o LUVs (red, 1,2-dipalmitoyl-*sn*-glycero-3-phosphocholine: DPPC). (B) FLIM images of **4** in L_d (top) and L_o GUVs (bottom, sphingomyelin/cholesterol: SM/CL). (C-F) Confocal images of HeLa Kyoto cells stained with PM **1** (C), Lyso **2** (D), ER **3** (E) and Mito Flipper **4** (F) (top), the respective trackers (middle), and the merged images (bottom); scale bars: 10 µm. (G) Fluorescence lifetime of **2**–**4** in HeLa Kyoto cells before (black) and after hypertonic osmotic shock (red).

a different, long and hydrophilic linker to enable the partitioning of the protein anchored probe in the membrane.[13,16] The synthesis of all probes is described in the SI (Schemes S1–S4).

Consistent with increasing planarization in the ground state, flippers **2**–**4** gave the expected red-shifted excitation maxima in solid-ordered (S_o) compared to liquid-disordered (L_d) membranes of large unilamellar vesicles (LUVs, Figures 2A, S1–S9, Table 1).[7,9,19–21] Also as expected were the higher average lifetimes τ of **2**–**4** in liquid-ordered (L_o) compared to L_d membranes in FLIM images of giant unilamellar vesicles (GUVs, Figures 2B, S11, Table 1).[5,19] Compared to the meticulously optimized original **1**[19] in ordered membranes (λ_{So} 490 nm, τ_{Lo} 6.4 ns), the new probes **2-4** showed overall smaller red shift of the excitation wavelength (λ_{So} 475 nm) and the lifetime (τ_{Lo} 5.5–5.8 ns), presumably due to less perfect positioning along the lipid tails in the membrane (Table 1).[7,22] These results confirmed that substitution of

the carboxylate in the new probes **2**–**4** is well tolerated without significant losses in mechanosensitivity.[20,21]

Intracellular targeting by probes **2**–**4** was studied using confocal microscopy. Co-localization of targeted flippers with their specific trackers[12–16] were excellent in both HeLa Kyoto (Figures 2D–2F, S12–S13, Table 1) and COS7 cells (Figures S14–S15). Characteristic staining patterns of organelles were also visible in FLIM images of probes **2**–**4** in standard HeLa (Figure S16) and more clearly in COS7 cells (Figure 3). COS7 cells treated with **3** revealed dense staining around the nucleus attributed to ER sheets, a thin meshwork attributed to tubular ER, and also the nuclear envelope (Figures 3B, S14, S19, S20). The average lifetimes were different for all probes in HeLa Kyoto cells (PM **1** > Lyso **2** > ER **3** > Mito **4**, Table 1, Figure 2G, black) and COS7 cells (Figure 3, black histograms, Table 1). All values were in-between the extremes measured in pure single-component model L_d and L_o membranes in GUVs. The variations in lifetimes originate mainly from differences in membrane organization (including contributions from lipid composition, microdomains, maybe also proteins, viscosity, etc),[5,9,10,23] and from the different mechanosensitivity of probes **1**-**4** (Figure 2A, Table 1). Thus, lifetimes in organelles at rest cannot be directly correlated to possible differences in membrane tension. However, the reduction of membrane tension by hypertonic shocks uniformly reduced lifetimes of probes in HeLa Kyoto cells (Figure 2G, red) and in COS7 cells (Figure 3, red histograms, Table 1). Decreasing lifetimes with decreasing tension was as with Flipper-TR® **1**[5] and thus consistent with operational probes reporting on tension-induced lipid reorganization in the membranes of the respective organelles (Figure 1B). Increasing counts in FLIM histograms with decreasing tension might originate from the increased amount of folded membrane in the focal plane upon cell shrinkage. Nevertheless, such intensity changes do not affect the fluorescence lifetime.

Hydrophilic Mito control **5** equipped with a mitochondria targeting unit co-localized with MitoTracker Red in HeLa cells, but failed to respond to the membrane tension change (Table 1, Figure S18). These results are consistent with the accumulation of this probe in the mitochondrial lumen. Further, viscosity-sensitive molecular rotors halo-tagged into the lumen responded to the osmotic shock in the opposite way to those of probes **2**-**4**.[12] These differences provided corroborative evidence that flippers **2**-**4** indeed localize in the organellar membranes and respond to changes in membrane tension with changes in fluorescence lifetime.

All organelles showed heterogeneous lifetime distributions. For instance, membranes of the tubular ER appeared more ordered (τ = 4.1 ns) than those of the ER sheets (τ = 3.5 ns) but responded equally to tension ($\Delta\tau \approx$ 0.4 ns, Figures 3B, S17). The lifetime of **3** in the nuclear membrane ($\tau \approx$3.4 ns) was similar to that in the ER sheets, consistent with their continuous nature (Figure S20).

Selected experiments beyond probe characterization were performed to outline the potential of intracellular tension probes in promoting new discoveries. For instance, co-labeling of Lyso Flipper **2** with fluorescently labeled epidermal growth factor[24] provided insights on endosomal trafficking (Alexa Fluor® 647 EGF, Figures 4A, S13).[25] After ten minutes, poor colocalization (around 20%) of the internalized EGF receptor (EGFR) in endosomes with probe **2** was observed. After two hours, the fluorescent EGF was mainly located in late-endosomes and lysosomes and showed increased overlapping with the Lyso Flipper **2**. This experiment indicated that probe **2** selectively accumulates in late endosomes and lysosomes. Replacement of morpholine in **2** by a more basic amine can be envisaged to allow targeting of less acidic compartments such as early endosomes.

Table 1. Mechanophore Characteristics.[a]

C [b]	λ_{So}[c] (nm)	λ_{Ld}[d] (nm)	τ_{Lo}[e] (ns)	τ_{Ld}[f] (ns)	PCC[g]	τ_i[h] (ns)	τ_h[i] (ns)	τ_i[h] (ns)	τ_h[i] (ns)
S	LUVs		GUVs		HeLa			COS7	
1[j]	490	435	6.4	3.8	-	4.8	4.2	-	-
2	475	437	5.6	3.1	0.9	3.7	3.3	3.9	3.6
3	475	436	5.8	3.0	0.9	3.4	3.0	3.5[k]	3.3
4	475	439	5.5	2.9	0.9	3.2	3.0	3.3	3.1
5	br[l]	br[l]	-	-	0.8	3.2	3.2	-	-

[a]Expanded version: Table S1. [b]Conditions; probes **1**-**5**: Figure 1; S: Systems. [c]Excitation maxima in S_o DPPC LUVs. [d]Same in L_d DOPC. [e]Average fluorescence lifetime in SM/CL 7:3 GUVs. [f]Same in DOPC. [g]Pearson's correlation coefficients determined using CLSM against LysoTracker (**2**), ER-Tracker (**3**), MitoTracker Red (**4**, **5**). [h]Average τ under isotonic conditions. [i]Same under hypertonic conditions. [j]Data from refs. 5 and 19; average τ re-calculated. [k]Examples for suborganellar heterogeneity ignored in average lifetimes: tubular ER: 4.1 ns, ER sheets: 3.5 ns, nuclear membrane: 3.4 ns. [l]Broad signals without distinct maxima.

As another example, the different lifetimes of probes **1**-**4** were exploited to simultaneously detect different organelles. Co-incubation of ER Flipper **3** and Mito Flipper **4** revealed their targets by the different fluorescence lifetime and intensity contrast: Mitochondria yielded higher signal intensity, whereas fluorescence lifetime of tension probes was higher in the tubular ER (Figures 4B, S19). Other cross-sections revealed different fluorescence lifetimes for the nuclear envelope, the ER and lysosomes (Figure S20).

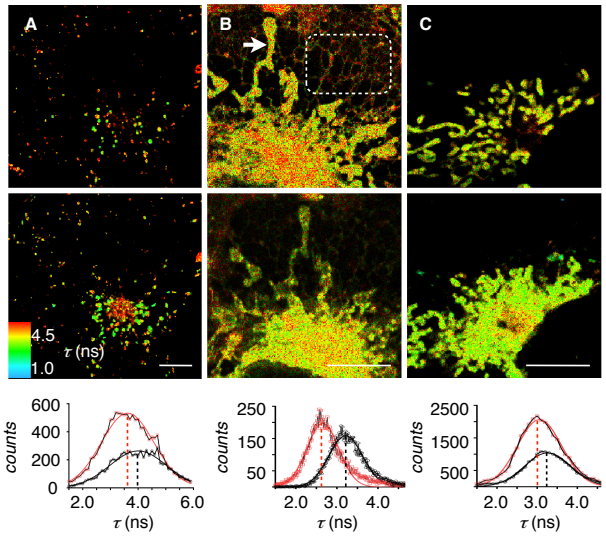

Figure 3. FLIM images of Lyso **2** (A), ER **3** (B, arrow: sheets, framed: tubules) and Mito **4** (C) in COS7 cells (1 µM, 20 min incubation) before (top) and after (middle) hypertonic osmotic shock, with corresponding lifetime histograms before (black) and after shock (red, bottom); scale bars: 10 µM.

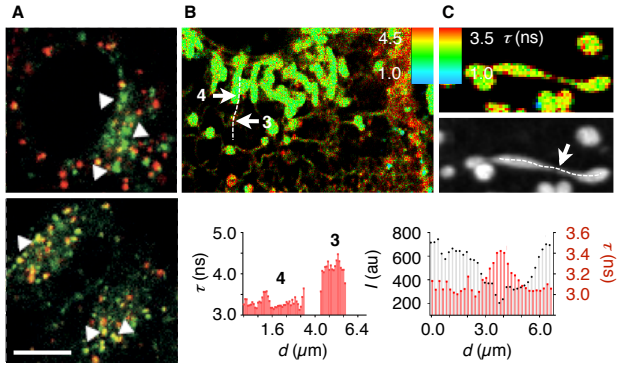

Figure 4. (A) Confocal image of Hela MZ cells incubated for 10 min with far red EGF (red) and Lyso flipper **2** (green; arrows indicate lack of co-localization, top) and of cells rinsed and chased for 2 h (arrows indicate co-localization, bottom), scale bar: 10 µm. (B) FLIM images of COS7 cells co-incubated with ER **3** and Mito flipper **4** (top), with lifetime along the indicated cross-section (bottom). (C) FLIM (top) and intensity images (middle) of COS7 cells incubated with Mito flipper **3**, with fluorescence intensity (black) and lifetime (red) along the indicated cross-section (bottom).

A striking example for a long-standing question that could not be answered without the new tension probes was provided by Mito Flipper **4** in COS7 cells (Figure 4C). Measurements of fluorescence inten-

sity and lifetime along sites of mitochondrial constrictions that precede fission[26] revealed that in the constricted area, the intensity decreases due to lower probe concentration, but lifetime increases, thus providing direct experimental evidence of the increased membrane tension during mitochondrial constriction. A complementary analysis on the role of membrane tension in mitochondrial fission using Mito Flipper **4** will be reported elsewhere.[27]

In conclusion, three organelle-selective fluorescent membrane tension probes were designed, synthesized and characterized both in vesicles and living cells. As proven by the sensitivity of their lifetime to osmotic shock, they report on changes in membrane tension and reveal different lifetimes for each target. These preliminary results promise important discoveries in future toward understanding of the intracellular membrane dynamics during biological events.

ASSOCIATED CONTENT

Supporting Information. Detailed experimental procedures. This material is available free of charge via the Internet at http://pubs.acs.org.

AUTHOR INFORMATION

Corresponding Authors

stefan.matile@unige.ch, aurelien.roux@unige.ch

Notes

Flipper-TR® is commercially available from Spirochrome, through the NCCR Store (https://nccr-chembio.ch/technologies/nccr-store/).

ACKNOWLEDGMENTS

We thank the NMR, MS and bioimaging platforms for services, and the University of Geneva, the Swiss National Centre of Competence in Research (NCCR) Chemical Biology, the NCCR Molecular Systems Engineering and the Swiss NSF for financial support.

REFERENCES

(1) (a) Leiphart, R. J.; Chen, D.; Peredo, A. P.; Loneker, A. E.; Janmey, P. A. Mechanosensing at Cellular Interfaces. *Langmuir* **2018**, in press, DOI: 10.1021/acs.langmuir.8b02841. (b) Krieg, M.; Fläschner, G.; Alsteens, D.; Gaub, B. M.; Roos, W. H.; Wuite, G. J. L.; Gaub, H. E.; Gerber, C.; Dufrêne, Y. F.; Müller, D. J. Atomic Force Microscopy-Based Mechanobiology. *Nat. Rev. Phys.* **2019**, *1*, 41–57. (c) Sens, P.; Plastino, J. Membrane Tension and Cytoskeleton Organization in Cell Motility. *J. Phys.*

Condens. Matter **2015**, *27*, 273103. (d) Diz-Muñoz, A.; Weiner, O. D.; Fletcher, D. A. In Pursuit of the Mechanics That Shape Cell Surfaces. *Nat. Phys.* **2018**, *14*, 648–652.

(2) Pontes, B.; Monzo, P.; Gauthier, N. C. Membrane Tension: A Challenging but Universal Physical Parameter in Cell Biology. *Semin. Cell Dev. Biol.* **2017**, *71*, 30–41.

(3) Roca-Cusachs, P.; Conte, V.; Trepat, X. Quantifying Forces in Cell Biology. *Nat. Cell Biol.* **2017**, *19*, 742–751.

(4) Feng, Q.; Kornmann, B. Mechanical Forces on Cellular Organelles. *J. Cell. Sci.* **2018**, *131*, jcs218479.

(5) Colom, A.; Derivery, E.; Soleimanpour, S.; Tomba, C.; Dal Molin, M.; Sakai, N.; González-Gaitán, M.; Matile, S.; Roux, A. A Fluorescent Membrane Tension Probe. *Nat. Chem.* **2018**, *10*, 1118–1125.

(6) (a) Barbarella, G.; Di Maria, F. Supramolecular Oligothiophene Microfibers Spontaneously Assembled on Surfaces or Coassembled with Proteins inside Live Cells. *Acc. Chem. Res.* **2015**, *48*, 2230–2241. (b) Cinar, M. E.; Ozturk, T. Thienothiophenes, Dithienothiophenes, and Thienoacenes: Syntheses, Oligomers, Polymers, and Properties. *Chem. Rev.* **2015**, *115*, 3036–3140.

(7) Dal Molin, M.; Verolet, Q.; Colom, A.; Letrun, R.; Derivery, E.; Gonzalez-Gaitan, M.; Vauthey, E.; Roux, A.; Sakai, N.; Matile, S. Fluorescent Flippers for Mechanosensitive Membrane Probes. *J. Am. Chem. Soc.* **2015**, *137*, 568–571.

(8) (a) Bauza, A.; Mooibroek, T. J.; Frontera, A. The Bright Future of Unconventional σ/π-Hole Interactions. *ChemPhysChem* **2015**, *16*, 2496–2517. (b) Vogel, L.; Wonner, P.; Huber, S. M. Chalcogen Bonding: An Overview. *Angew. Chem. Int. Ed.* **2018**, in press, DOI: 10.1002/anie.201809432. (c) Beno, B. R.; Yeung, K. S.; Bartberger, M. D.; Pennington, L. D.; Meanwell, N. A. A Survey of the Role of Noncovalent Sulfur Interactions in Drug Design. *J. Med. Chem.* **2015**, *58*, 4383–438. (d) Macchione, M.; Tsemperouli, M.; Goujon, A.; Mallia, A. R.; Sakai, N.; Sugihara, K.; Matile, S. Mechanosensitive Oligodithienothiophenes: Transmembrane Anion Transport Along Chalcogen-Bonding Cascades. *Helv. Chim. Acta* **2018**, *101*, e1800014.

(9) Humeniuk, H. V.; Rosspeintner, A.; Licari, G.; Kilin, V.; Bonacina, L.; Vauthey, E.; Sakai, N.; Matile, S. White-Fluorescent Dual-Emission Mechanosensitive Membrane Probes That Function by Bending Rather than Twisting. *Angew. Chem. Int. Ed.* **2018**, *57*, 10559–10563.

(10) (a) Klymchenko, A. S. Solvatochromic and Fluorogenic Dyes as Environment-Sensitive Probes: Design and Biological Applications. *Acc. Chem. Res.* **2017**, *50*, 366–375. (b) Xiong, Y.; Vargas Jentzsch, A.; Osterrieth, J. W. M.; Sezgin, E.; Sazanovich, I. V.; Reglinski, K.; Galiani, S.; Parker, A. W.; Eggeling, C.; Anderson, H. L. Spironaphthoxazine Switchable Dyes for Biological Imaging. *Chem. Sci.* **2018**, *9*, 3029–3040. (c) Kulkarni, R. U.; Miller, E. W. Voltage Imaging: Pitfalls and Potential. *Biochemistry*

2017, *56*, 5171–5177. (d) Haidekker, M. A.; Theodorakis, E. A. Ratiometric Mechanosensitive Fluorescent Dyes: Design and Applications. *J. Mater. Chem. C* **2016**, *4*, 2707–2718. (e) Muraoka, T. Umetsu, K.; Tabata, K. V.; Hamada, T.; Noji, H.; Yamashita, T.; Kinbara, K. Mechano-Sensitive Synthetic Ion Channels. *J. Am. Chem. Soc.* **2017**, *139*, 18016–18023. (f) Kubankova, M.; Lopez Duarte, I.; Kiryushko, D.; Kuimova, M. K. Molecular Rotors Report on Changes of Live Cell Plasma Membrane Microviscosity upon Interaction with Beta-Amyloid Aggregates. *Soft Matter* **2018**, *14*, 9466–9474.

(11) (a) Niko, Y.; Didier, P.; Mely, Y.; Konishi, G.; Klymchenko, A. S. Bright and Photostable Push-Pull Pyrene Dye Visualizes Lipid Order Variation between Plasma and Intracellular Membranes. *Sci. Rep.* **2016**, *6*, 18870. (b) Mazeres, S.; Fereidouni, F.; Joly, E. Using Spectral Decomposition of the Signals from Laurdan-Derived Probes to Evaluate the Physical State of Membranes in Live Cells. *F1000Research* **2017**, *6*, 763. (c) Zhang, H.; Fan, J.; Dong, H.; Zhang, S.; Xu, W.; Wang, J.; Gao, P.; Peng, X. Fluorene-Derived Two- Photon Fluorescent Probes for Specific and Simultaneous Bioimaging of Endoplasmic Reticulum and Lysosomes: Group-Effect and Localization. *J. Mater. Chem. B* **2013**, *1*, 5450–5455. (d) Iaea, D. B.; Maxfield, F. R. Membrane Order in the Plasma Membrane and Endocytic Recycling Compartment. *PLoS One* **2017**, *12*, e0188041.

(12) Chambers, J. E.; Kubánková, M.; Huber, R. G.; López-Duarte, I.; Avezov, E.; Bond, P. J.; Marciniak, S. J.; Kuimova, M. K. An Optical Technique for Mapping Microviscosity Dynamics in Cellular Organelles. *ACS Nano* **2018**, *12*, 4398–4407.

(13) (a) Wagner, N.; Stephan, M.; Höglinger, D.; Nadler, A. A Click Cage: Organelle-Specific Uncaging of Lipid Messengers. *Angew. Chem. Int. Ed.* **2018**, *57*, 13339–13343. (b) Zhu, H.; Fan, J.; Du, J.; Peng, X. Fluorescent Probes for Sensing and Imaging within Specific Cellular Organelles. *Acc. Chem. Res.* **2016**, *49*, 2115–2126. (c) Xu, W.; Zeng, Z.; Jiang, J.-H.; Chang, Y.-T.; Yuan, L. Discerning the Chemistry in Individual Organelles with Small-Molecule Fluorescent Probes. *Angew. Chem. Int. Ed.* **2016**, *55*, 13658–13699. (d) Su, D.; Teoh, C. L.; Wang, L.; Liu, X.; Chang, Y.-T. Motion-Induced Change in Emission (MICE) for Developing Fluorescent Probes. *Chem. Soc. Rev.* **2017**, *46*, 4833–4844.

(14) (a) Wallabregue, A.; Moreau, D.; Sherin, P.; Moneva Lorente, P.; Jarolímová, Z.; Bakker, E.; Vauthey, E.; Gruenberg, J.; Lacour, J. Selective Imaging of Late Endosomes with a pH-Sensitive Diazaoxatriangulene Fluorescent Probe. *J. Am. Chem. Soc.* **2016**, *138*, 1752–1755. (b) Li, L.-L.; Li, K.; Li, M.-Y.; Shi, L.; Liu, Y.-H.; Zhang, H.; Pan, S.-L.; Wang, N.; Zhou, Q.; Yu, X.-Q. BODIPY-Based Two-Photon Fluorescent Probe for Real-Time Monitoring of Lysosomal Viscosity with Fluorescence Lifetime Imaging Microscopy. *Anal. Chem.* **2018**, *90*, 5873–5878.

(15) (a) Guo, R.; Yin, J.; Ma, Y.; Wang, Q.; Lin, W. A Novel Mitochondria-Targeted Rhodamine Analogue for the Detection of Viscosity Changes in Living Cells, Zebra Fish and Living Mice. *J. Mater.*

Chem. B **2018**, *6*, 2894–2900. (b) Bauer, C.; Duwald, R.; Labrador, G. M.; Pascal, S.; Moneva Lorente, P.; Bosson, J.; Lacour, J.; Rochaix, J.-D. Specific Labeling of Mitochondria of *Chlamydomonas* with Cationic Helicene Fluorophores. *Org. Biomol. Chem.* **2018**, *16*, 919–923. (c) Feng, S.; Harayama, T.; Montessuit, S.; David, F. P.; Winssinger, N.; Martinou, J.-C.; Riezman, H. Mitochondria-Specific Photoactivation to Monitor Local Sphingosine Metabolism and Function. *eLife* **2018**, *7*, e34555. (d) Yang, Z.; He, Y.; Lee, J.-H.; Park, N.; Suh, M.; Chae, W.-S.; Cao, J.; Peng, X.; Jung, H.; Kang, C.; Kim, J. S. A Self-Calibrating Bipartite Viscosity Sensor for Mitochondria. *J. Am. Chem. Soc.* **2013**, *135*, 9181–9185. (e) Leung, C. W. T.; Hong, Y.; Chen, S.; Zhao, E.; Lam, J. W. Y.; Tang, B. Z. A Photostable AIE Luminogen for Specific Mitochondrial Imaging and Tracking. *J. Am. Chem. Soc.* **2013**, *135*, 62–65. (f) Jiménez-Sánchez, A.; Lei, E.; Kelley, S. O. A Multifunctional Chemical Probe for Local Micropolarity and Microviscosity in Mitochondria. *Angew. Chem. Int. Ed.* **2018**, *57,* 8891–8895.

(16) (a) Halabi, E. A.; Püntener, S.; Rivera-Fuentes, P. A Simple Probe for Super-Resolution Imaging of the Endoplasmic Reticulum in Living Cells. *Helv. Chim. Acta* **2018**, *101*, e1800165. (b) Ghosh, S.; Nandi, S.; Ghosh, C.; Bhattacharyya, K. Fluorescence Dynamics in the Endoplasmic Reticulum of a Live Cell: Time-Resolved Confocal Microscopy. *ChemPhysChem* **2016**, *17*, 2818–2823. (c) Meinig, J. M.; Fu, L.; Peterson, B. R. Synthesis of Fluorophores that Target Small Molecules to the Endoplasmic Reticulum of Living Mammalian Cells. *Angew. Chem. Int. Ed.* **2015**, *54*, 9696–9699.

(17) (a) Ho, J. C. S.; Rangamani, P.; Liedberg, B.; Parikh, A. N. Mixing Water, Transducing Energy, and Shaping Membranes: Autonomously Self-Regulating Giant Vesicles. *Langmuir* **2016**, *32*, 2151–2163. (b) Chen, D.; Santore, M. M. Three Dimensional (Temperature–Tension–Composition) Phase Map of Mixed DOPC–DPPC Vesicles: Two Solid Phases and a Fluid Phase Coexist on Three Intersecting Planes. *Biochim. Biophys. Acta* **2014**, *1838*, 2788–2797. (c) Hamada, T.; Kishimoto, Y.; Nagasaki, T.; Takagi, M. Lateral Phase Separation in Tense Membranes. *Soft Matter* **2011**, *7*, 9061–9068. (d) Baumgart, T.; Hess, S. T.; Webb, W. W. Imaging Coexisting Fluid Domains in Biomembrane Models Coupling Curvature and Line Tension. *Nature* **2003**, *425*, 821–824.

(18) Riggi, M.; Niewola-Staszkowska, K.; Chiaruttini, N.; Colom, A.; Kusmider, B.; Mercier, V.; Soleimanpour, S.; Stahl, M.; Matile, S.; Roux, A.; Loewith, R. Decrease in Plasma Membrane Tension Triggers PtdIns(4,5)P_2 Phase Separation to Inactivate TORC2. *Nat. Cell Biol.* **2018**, *20*, 1043–1051.

(19) Soleimanpour, S.; Colom, A.; Derivery, E.; Gonzalez-Gaitan, M.; Roux, A.; Sakai, N.; Matile, S. Headgroup Engineering in Mechanosensitive Membrane Probes. *Chem. Commun.* **2016**, *52*, 14450–14453.

(20) Strakova, K.; Soleimanpour, S.; Diez-Castellnou, M.; Sakai, N.; Matile, S. Ganglioside-Selective Mechanosensitive Fluorescent Membrane Probes. *Helv. Chim. Acta* **2018**, *101*, e1800019.

(21) Goujon, A.; Straková, K.; Sakai, N.; Matile, S. Streptavidin Interfacing as a General Strategy to Localize Fluorescent Membrane Tension Probes in Cells. *Chem. Sci.* **2019**, *10*, 310–319.

(22) Neuhaus, F.; Zobi, F.; Brezesinski, G.; Dal Molin, M.; Matile, S.; Zumbuehl, A. Correlation of Surface Pressure and Color Hue of Planarizable Push-Pull Chromophores at the Air/Water Interface. *Beilstein J. Org. Chem.* **2017**, *13*, 1099–1105.

(23) (a) van Meer, G.; Voelker, D. R.; Feigenson, G. W. Membrane Lipids: Where They Are and How They Behave. *Nat. Rev. Mol. Cell Biol.* **2008**, *9*, 112–124. (b) Jackson, C. L.; Walch, L.; Verbavatz, J.-M. Lipids and Their Trafficking: An Integral Part of Cellular Organization. *Dev. Cell* **2016**, *39*, 139–153.

(24) (a) Henriksen, L.; Grandal, M. V.; Knudsen, S. L. J.; van Deurs, B.; Grøvdal, L. M. Internalization Mechanisms of the Epidermal Growth Factor Receptor after Activation with Different Ligands. *PLoS One* **2013**, *8*, e58148. (b) Orth, J. D.; Krueger, E. W.; Weller, S. G.; McNiven, M. A. A Novel Endocytic Mechanism of Epidermal Growth Factor Receptor Sequestration and Internalization. *Cancer Res.* **2006**, *66*, 3603–3610.

(25) (a) Doherty, G. J.; McMahon, H. T. Mechanisms of Endocytosis. *Annu. Rev. Biochem.* **2009**, *78*, 857–902. (b) Barbieri, E.; Di Fiore, P. P.; Sigismund, S. Endocytic Control of Signaling at the Plasma Membrane. *Curr. Opin. Cell Biol.* **2016**, *39*, 21–27.

(26) (a) Archer, S. L. Mitochondrial Dynamics – Mitochondrial Fission and Fusion in Human Diseases. *N. Engl. J. Med.* **2013**, *369*, 2236–2251. (b) van der Bliek, A. M.; Shen, Q.; Kawajiri, S. Mechanisms of Mitochondrial Fission and Fusion. *Cold Spring Harbor Perspect. Biol.* **2013**, *5*, a011072. (c) Youle, R. J.; van der Bliek, A. M. Mitochondrial Fission, Fusion, and Stress. *Science*, **2012**, *337*, 1062–1065.

(27) Mahecic, D.; Carlini, L.; Kleele, T.; Colom, A.; Goujon, A.; Matile, S.; Roux, A.; Manley, S. Membrane Bending Energy and Tension Govern Mitochondrial Division. Submitted.

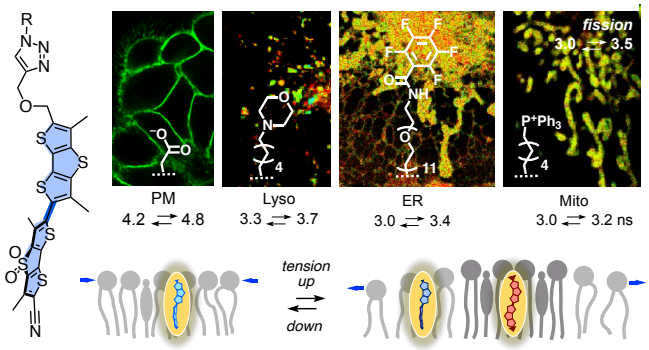
PM
4.2 ⇄ 4.8
Lyso
3.3 ⇄ 3.7
ER
3.0 ⇄ 3.4
fission
3.0 ⇄ 3.5
Mito
3.0 ⇄ 3.2 ns
tension
up
down